Journal of the Geological Survey of Brazil vol 7, n3, 277 - 288, December 2024

Journal of the Geological Survey of Brazil

Geochemistry of serpentinites from the central portion of the Rio Piranhas-Seridó Domain, Borborema Province, Northeastern Brazil: Implications for genesis and geotectonic setting

Frank Gurgel Santos[1*], Mário Tavares de Oliveira Cavalcanti Neto[2], Valderez Pinto Ferreira[3], Anelise L. Bertotti[3]

[1]SGB-CPRM - Serviço Geológico do Brasil, Superintendência Regional do Recife (SUREG-RE), Avenida Sul, 2291, Afogados, Recife, Pernambuco, Brasil. CEP: 50.770-011
[2]Instituto Federal de Educação, Ciência e Tecnologia do Rio Grande do Norte – IFRN, Campus Natal Central, Avenida Senador Salgado Filho, 1559, Tirol, Natal, Rio Grande do Norte, Brasil. CEP: 59015-000
[3]Universidade Federal de Pernambuco – UFPE, Centro de Tecnologia e Geociências, Departamento de Geologia, Avenida da Arquitetura, s/n, Cidade Universitária, Recife, PE, Brasil. CEP: 50740-550

Abstract

The mineralogical and geochemical composition of serpentinites aids in identifying the tectonic and metamorphic processes that have altered these rocks throughout geological time. Their ultrabasic and komatiitic signature can be linked to the high-temperature and high-pressure conditions present during the formation of the protolith. The serpentinites in the central portion of the Rio Piranhas-Seridó Domain, located in the northeastern extreme of the Borborema Province, are observed in the Serra Verde and Oiticica mines near the town of São Tomé, in the State of Rio Grande do Norte. These rocks occur as elongated ellipsoidal bodies (300 x 50 m) tectonically embedded within the Paleoproterozoic gneisses of the Caicó Complex and within the Neoproterozoic paragneisses and schists of the Seridó Group. They are melanocratic, fine-grained rocks with a greenish color and foliation aligned with the regional NE-SW trend. The essential mineral is serpentine, which replaces the iron and magnesium minerals of the protolith, with chlorite, tremolite, quartz, and magnetite occurring as accessory phases. Major, minor, and trace chemical elements suggest an ultrabasic composition, indicating olivine as the primary mineral. Despite the effects of metamorphic processes, the rock still retains the predominant chemistry of the protolith. The high magnesium content points to a komatiitic signature, implying high temperature, high pressure, and a high degree of partial melting in the genesis of the protolith. Serpentinites are not common lithotypes; therefore, this publication, one of the few addressing the topic, aims to report the occurrence of these rare lithotypes. Through chemical analyses and the evaluation of mineralogical transformations, these rocks display characteristics compatible with those of a greenstone belt, which has been disrupted by the action of shear zones with significant implications for the geodynamic setting of the region.

Article Information

Publication type: Research Papers
Received 6 September 2024
Accepted 22 November 2024
Online pub. 5 December 2024
Editor: E.Klein

Keywords:
Archean
Ultramafic Rocks
Northern Borborema Province
Geochemistry
Greenstone Belt

*Corresponding author
Frank Gurgel Santos
E-mail address: frank.santos@sgb.gov.br

1. Introduction

In the central portion of the Rio Piranhas-Seridó Domain, located in the northeastern extreme of the Borborema Province, serpentinites are associated with gneisses of the Caicó Complex and paragneisses/micaschists of the Seridó Group (Figure 1). In other areas of the Borborema Province, they typically occur in very restricted forms, composing mafic-ultramafic sequences in contact with granites and gneisses (Santos et al. 2014; Uchoa Filho et al. 2014; Pitombeira et al. 2016; Ferreira et al. 2020a, 2020b).

Serpentinites are rocks that consist primarily of minerals from the serpentine group, which are formed by the hydration of ultramafic rocks, where the main Mg-rich minerals (olivine and pyroxenes) are replaced by hydrated magnesium silicate minerals (serpentines; Evans et al. 2013). These lithotypes are produced in a wide range of geological contexts and ages, being found in hydrothermal systems of oceanic floors, mid-ocean ridges, orogenic belts, and mantle plumes (Evans et al. 2013; Grove and Parman 2004). However, as most reported occurrences are Archean in age, modern environments (such as oceanic floor faults and subduction zones) are unlikely, given that the thermal and tectonic regimes differ significantly from those proposed for early Earth.

These rocks are challenging to interpret in terms of petrogenesis, as their primary mineralogy is rarely preserved

ISSN: 2595-1939
https://doi.org/10.29396/jgsb.2024.v7.n3.4
Open access at https://jgsb.sgb.gov.br

due to the hydration process that alters the original rock composition (Szilas et al. 2014). Some major and minor elements (Mg, Fe, Al, Ca, Na, K, P, Mn, Ti, Ni, Cr) of the protolith tend to be preserved during hydration processes when the primary mineral phase is olivine. In contrast, rare earth elements (REE) and other trace elements are influenced by fluid-rock interaction, their content in primary phases, and their stability during hydration, as well as their affinity with secondary minerals (Deschamps et al. 2013; O'Hanley 1996; Bogolepov 1970; Coleman and Keith 1971).

(Meta)ultramafic bodies with a geochemical signature of komatiites (MgO > 18%) are frequently found in volcanic rock successions within most greenstone belts, yet they remain quite rare, typically representing less than 10% of the total volume of these associations (De Wit and Ashwal 1997). In addition to serving as an important window into the primitive mantle and providing significant implications for thermal evolution models of the Earth, komatiites are of economic interest due to their association with major nickel and gold deposits in greenstone belts in Australia, Canada, and South Africa (Dostal 2008).

Mineral deposits (tungsten, gold, tantalite-columbite, iron, gemstones, etc.) in the study area have been known since the 1940s and are mostly temporally and spatially associated with plutons of the Brasiliano igneous suite and/or shear zones acting as fluid conduits (Souza Neto et al. 2008). The interaction between serpentinites and Brasiliano granites in the study area is already recognized as responsible for the emerald mineralization at the Serra Verde Mine (Figure 1 and 2). The abrupt contacts between pegmatitic and phlogopite-rich bodies with serpentinite clearly indicate that metasomatic reactions with the ultramafic rocks played a crucial role in bringing together the key elements for emerald formation (Cr from the ultramafic rocks, and Be, Al, and Si from the pegmatites) (Zwaan et al. 2012; Santiago et al. 2019).

As these are uncommon lithotypes, rarely documented in the regional geological literature, associated with economically significant mineralization, and reported as the oldest rocks in South America (Santos et al. 2020), it is essential to highlight their discovery and deepen the understanding of these serpentinites. To achieve this, chemical analyses of major, minor, and trace elements were conducted to characterize their geochemistry. This study aims to enhance the understanding of metasomatic processes and the concentration of key elements, providing crucial information for future research on the genesis and economic potential of the associated mineralizations.

2. Geotectonic context

The Borborema Province (Almeida et al. 1981) comprises the northeastern portion of the South American platform and resulted from the tectonic convergence of the West African-São Luís and São Francisco-Congo cratons (Caby 1989; Brito Neves et al. 2000; Arthaud et al. 2008), as part of the consolidation of West Gondwana (Figure 1A). This province is located in the northeastern edge of Brazil and is bounded to the south by the São Francisco Craton, to the west by the Parnaíba Basin, and to the north and east by the Coastal Province.

The Borborema Province consists of an Archean to Paleoproterozoic gneiss-migmatite basement overlain by supracrustal sequences, all intruded by numerous Neoproterozoic granitoids (Jardim de Sá 1994; Souza et al. 2007, 2015). It is segmented by a complex Neoproterozoic system of high-temperature, crustal-scale shear zones (Jardim de Sá 1994), which define a configuration of independent tectonic domains. Generally, the Borborema Province is divided into three major subprovinces (Figure 1B): the External or Southern Subprovince, located between the Pernambuco Lineament and the São Francisco Craton; the Transversal Zone or Central Sector, situated between the Pernambuco and Patos Lineaments; and the Northern Subprovince, located north of the Patos Lineament. The Northern Subprovince includes the São José de Campestre, Rio Piranhas-Seridó, Jaguaribeano, Ceará Central, and Médio Coreaú domains (Delgado et al. 2003; Angelim et al. 2006; Medeiros et al. 2017).

The study area (Figure 1D) lies within the limits of the Rio Piranhas-Seridó Domain, whose basement is composed of rocks from the Caicó Complex. This complex includes Paleoproterozoic metavolcanic and metasedimentary rocks, dated to 2.15–2.20 Ga (Rb-Sr, Souza et al. 2007), such as metabasalts, amphibolite gneisses, intermediate-felsic tuffs, and sillimanite-muscovite-garnet-biotite gneisses, as well as metaplutonic rocks (gabbros, tonalites, granodiorites, and granites) metamorphosed to upper amphibolite to granulite facies near plutonic intrusions (Jardim de Sá 1994; Souza et al. 2007). This basement is overlain by rocks of the Seridó Group, which encompasses a Neoproterozoic supracrustal sequence, dated to 0.65–0.61 Ga (U-Pb SHRIMP, Van Schmus et al. 2003). The sequence includes the Jucurutu Formation at the base (dominantly paragneisses intercalated with marbles, quartzites, calc-silicate rocks, metaconglomerates, metavolcanic rocks, and iron formations), quartzites and metaconglomerates of the Equador Formation in the intermediate portion, and muscovite-biotite schists of the Seridó Formation at the top (with diverse intercalations of marbles, metavolcanic rocks, calc-silicate rocks, and metaconglomerates) (Jardim de Sá 1994). The Rio Piranhas-Seridó Domain witnessed significant Ediacaran magmatism during the Brasiliano orogeny, marked by massive plutonism with a wide compositional range occurring between 0.6 and 0.5 Ga (U-Pb, Rb-Sr, and Sm-Nd, Nascimento et al. 2015) (Jardim de Sá 1994; Souza et al. 2015).

The Rio Piranhas-Seridó Domain is characterized by three deformational events that shaped the structures imprinted on the rocks. The first event (D1) is associated with the formation of gneissic banding, restricted to the Rhyacian orthogneisses of the Caicó Complex. The D2 event generated isoclinal to intrafolial folds with strong transposition, followed by a tangential kinematic event. The final tectonometamorphic event (D3) was marked by transcurrent to oblique shear zones and the emplacement of late Neoproterozoic (Brasiliano) granitoids. The associated metamorphism ranges from upper amphibolite to granulite facies near plutonic intrusions and crustal-scale shear zones to greenschist facies in more distal areas (Jardim de Sá 1994; Souza et al. 2007).

The serpentinites outcropping near the city of São Tomé, in the state of Rio Grande do Norte (Figure 1C), occur as discontinuous lenses up to 300 meters long, aligned with the regional NNE-trending foliation. These lithotypes are embedded within the gneisses and migmatites of the Caicó Complex and the metasedimentary rocks of the Seridó Group, having been strongly affected by regional shear zones.

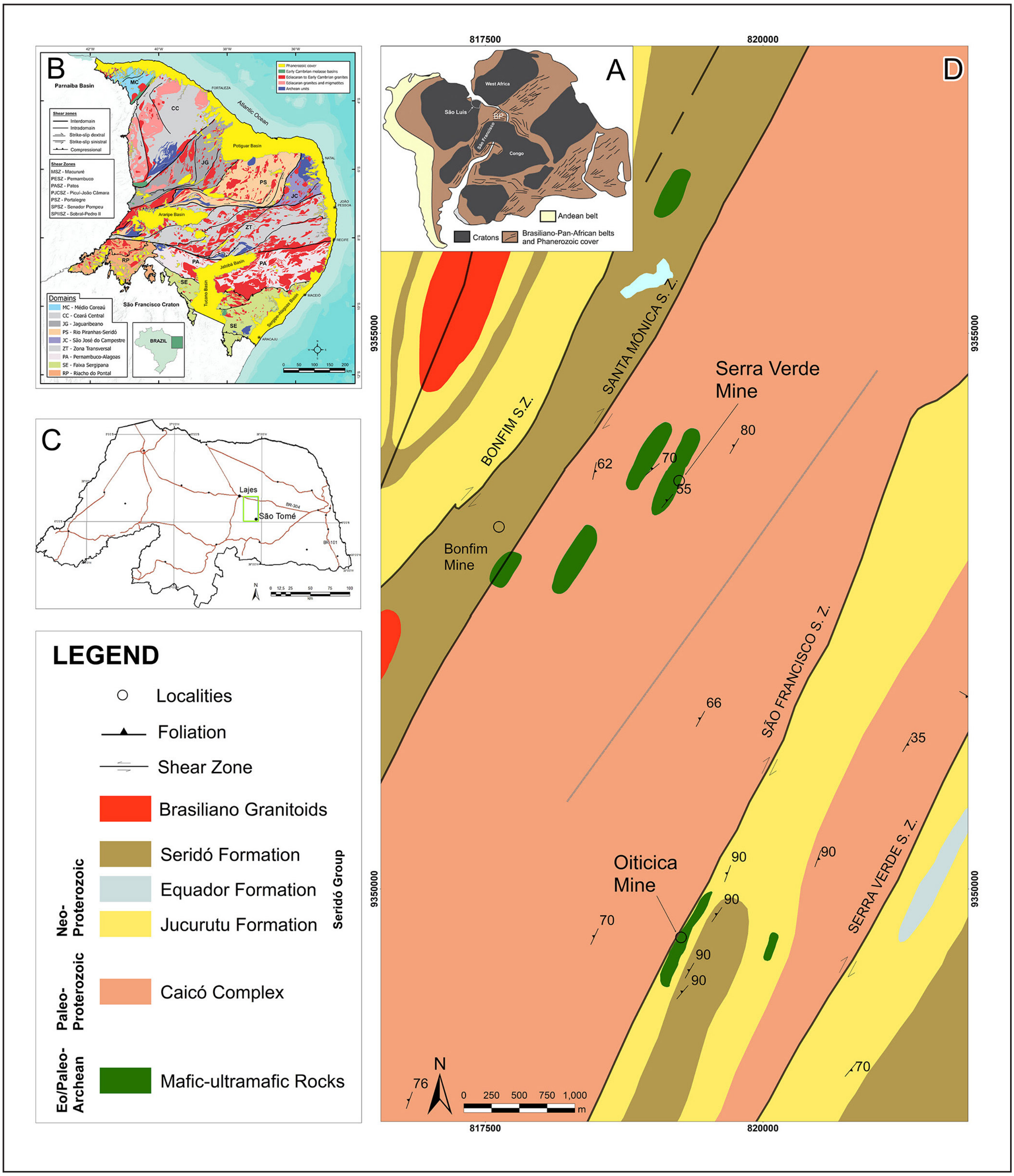

FIGURE 1. A. Pre-drift reconstruction of South America and Africa within the Gondwana supercontinent; BLocation of the study area within the Borborema Province (modified from Medeiros et al. 2017).; C. Study area location and nearby cities Lajes and São Tomé in the state of Rio Grande do Norte; D. Geological map of the study area.

3. Materials and Methods

Seven serpentinite samples (whole rock) were chemically analyzed at Acme Labs™ (Vancouver, Canada) using analytical packages 4A and 4B. In package 4A, the concentrations of major oxides and thirty-one minor elements were determined by Inductively Coupled Plasma Emission Spectrometry (ICP-ES). Sample preparation involved separating a 0.2-gram portion from each sample for fusion with lithium metaborate/tetraborate, with the resulting melt being rapidly digested in a nitric acid solution. Loss on Ignition (LOI) was determined by the difference in sample weights before and after being subjected to a temperature of 1000°C. Package 4B complemented 4A by determining the concentrations of rare earth and refractory elements using Inductively Coupled Plasma Mass Spectrometry (ICP-MS). The results are shown in Table 1.

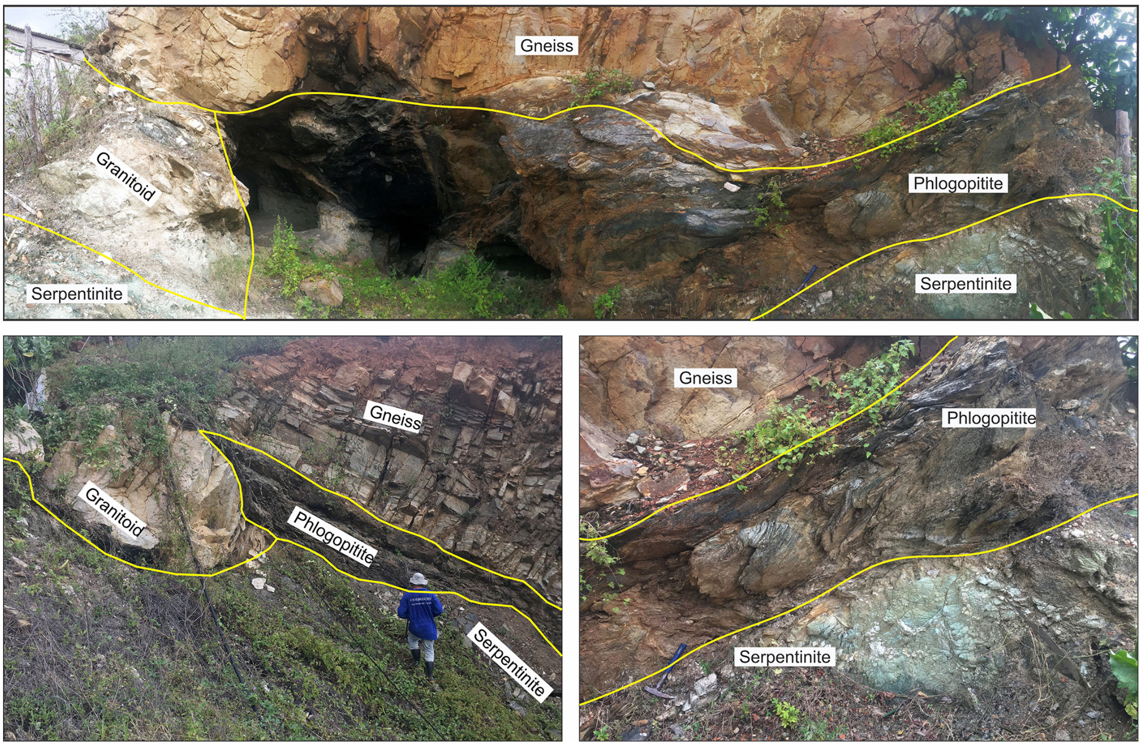

FIGURE 2 Field relationship of the serpentinite with the host rocks at Serra Verde Mine.

4. Results

4.1 Field Characteristics and Petrography

The serpentinites (Figure 3) occur as small lenticular bodies, elongated or rounded, in the central-northern part of the study area, as observed in the Serra Verde emerald mine (Figure 3A) and in an old scheelite exploration trench at the Oiticica mine (Figure 3B), both located near the city of São Tomé. The serpentinite lenses are always less than 300 meters in length and 50 meters in width, arranged discontinuously along the regional foliation over an approximate distance of 5 kilometers.

Serpentinites are generally melanocratic, fine-grained rocks, sometimes displaying elongated serpentine grains up to 1.0 cm in length. The rocks typically exhibit a greenish color when unaltered, primarily due to the high abundance of serpentine. Serpentine is the main phase (75–99%) in the lithotypes from both localities, occurring as a replacement for the primary ferromagnesian minerals of the protolith and forming micrometric veins filled with magnetite. In the serpentinites from the Serra Verde mine, accessory minerals include chlorite (<2%) and magnetite (<1%). In contrast, the serpentinites from the Oiticica mine show a more diverse mineralogical composition, containing tremolite (<2%), magnetite (<3%), and exsolved quartz (<3%). These minerals occur as xenoblastic crystals, exhibiting irregular contacts with serpentine, while magnetite also fills fractures in the rock (Figure 4).

Mafic-ultramafic lithotypes reported in the vicinity (tremolitites, chlorite-talc schists, and metapyroxenites) represent a petrographic variation that may result from different

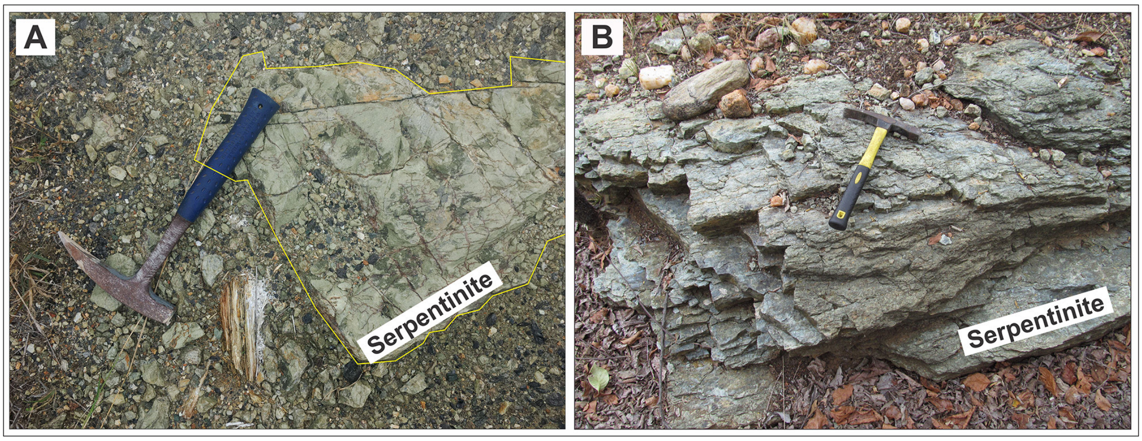

FIGURE 3. A. Serpentinite from the Serra Verde Mine, Coordinates (UTM 24M) X: 819254 e Y: 9349535; B. Serpentinite from the Oiticica Mine, Coordinates (UTM 24M) X: 819228 e Y: 9353606.

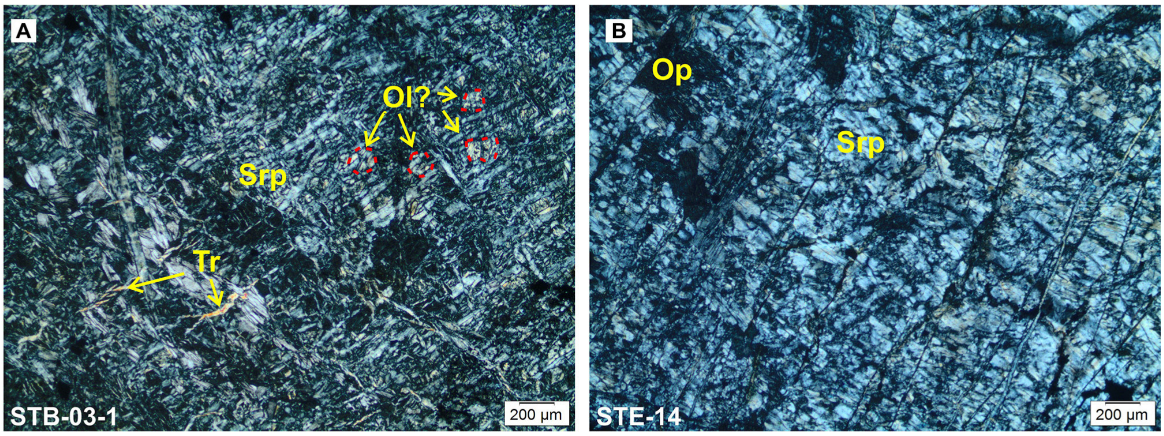

FIGURE 4. A. Photomicrography of serpentinite: A. Photomicrograph of serpentinite from the Oiticica Mine, transmitted light, N X; B. Photomicrograph of serpentinite from the Serra Verde Mine, transmitted light, N X. Mineral annotations: Srp = Serpentine, Op = Magnetite, Tr = Tremolite, Ol = Olivine.

degrees of hydrothermal alteration in similar protoliths. Fluid phases (K-P-H_2O-Ca-Na and H_2O-NaCl-CH_4-CO_2) identified in phlogopite crystals within the study area indicate the influence of granite intrusions, with fluids channeled through the significant shear zones active in the region (Santos et al. 2020; Ruiz et al. 2018; Santiago et al. 2019). These features suggest metamorphic processes, while the presence of phlogopitites at the Serra Verde Mine further supports the occurrence of metasomatism.

4.2. Lithogeochemistry

The chemical compositions of the serpentinites are presented in Table 1 and the graphs below, based on the collection sites at the Oiticica and Serra Verde mines. The rock analyses revealed SiO_2 values ranging from 35.72% to 43.48%, MgO from 28.88% to 34.63%, Fe_2O_3 from 7.08% to 11.29%, Al_2O_3 from 1.04% to 3.42%, TiO_2 from 0.02% to 0.05%, CaO from 0.05% to 2.53%, K_2O from 0.01% to 0.20%, Na_2O from 0.01% to 0.03%, and LOI from 12.4% to 16.9%. Binary plots of MgO vs. major element oxides (Figure 5) do not show distinctions between the serpentinites from the two mines, with no clear correlation trends. In general, the serpentinites from the Oiticica and Serra Verde mines exhibit similar behavior for major element oxides. However, some samples from the Oiticica mine display higher contents of CaO, K_2O, P_2O_3, FeO_t, and Cr_2O_3, while at the Serra Verde mine, some samples have higher Al_2O_3 contents. SiO_2 and TiO_2 values did not show any clear distinction between the two locations.

Diagrams with molecular ratio proportions involving magnesium, silicon, and aluminum were constructed to evaluate whether the initial composition of the studied serpentinites was disrupted.

In the MgO/Al_2O_3 vs. SiO_2/Al_2O_3 diagram (Pearce 1968, 1970) (Figure 6), two linear trends can be identified for the studied serpentinite samples. One trend is closely aligned with the olivine slope (1:4), while the other trend (1:0) does not approach the arrow indicating augite fractionation. This suggests that olivine constituted a fundamental fractionation phase in these rocks, and the chemical analysis results likely still reflect the original composition of the protolith.

In the trace element diagram normalized to the primitive mantle according to McDonough and Sun (1995), a pattern is observed with strong positive peaks for U and Pb and moderate negative peaks for Sr and Ti. The LILE elements show slight enrichment relative to the primitive mantle, while the HFSE elements are depleted (Figure 7A). The Oiticica Mine exhibits slightly more variability in certain points of the graph, with minor enrichment in elements such as P, Zr, Ta, and La compared to the Serra Verde Mine. However, overall, both mines follow similar patterns, suggesting they share analogous geological processes.

In the rare earth element (REE) diagram normalized to chondrites (Figure 7B) according to McDonough and Sun (1995), a near-horizontal pattern is observed, without prominent anomalies, and with concentrations lower than the primitive mantle, except for La and Ce, which are more enriched, creating a slightly fractionated pattern. Samples from the Oiticica Mine show a slight enrichment trend in light REEs (such as La and Ce) and fluctuations in heavier REEs (such as Dy and Yb). In contrast, samples from the Serra Verde Mine exhibit a less varied pattern, with some pronounced depletions in specific elements (such as Eu and Lu), indicating possible differentiation or selective depletion during geological processes.

5. Discussion

5.1 Chemical Composition: Influence of Hydrothermal/ Metasomatic Processes and the Relationship with Mineral Deposits

The mineralogy identified through thin sections and field observations (serpentine, chlorite, tremolite, muscovite, magnetite) suggests metamorphism consistent with the greenschist facies. The dispersion observed in the major and trace element diagrams (Figures 5, 6, and 7) indicates some disruption of the rock's original chemistry caused by metasomatism. Such processes have already been reported in other mafic-ultramafic rocks in the region (Zwaan et al. 2012; Santiago et al. 2019; Ruiz et al. 2018; Ferreira et al. 2020a, 2020b; Santos et al. 2020).

The enrichment in incompatible elements (U, Pb, and Ta) (Figure 7A) and disturbances in the Eu content

TABLE 1. Chemical Composition (ICP-ES) of Serpentinites Sampled from the Oiticica and Serra Verde Mines

	Oiticica mine				**Serra Verde mine**		
	STB-03	STB-03C	STB-03D	STC-14C2	STE-14	STE-14B	AM-7C
SiO_2 (wt. %)	43.48	35.72	43.25	36.53	39.62	42.95	36.69
MgO	30.27	33.59	30.12	28.88	33.10	30.36	34.63
Al_2O_3	1.04	1.23	1.24	3.42	1.34	1.19	1.37
Cr_2O_3	0.65	1.22	1.06	1.64	0.97	1.06	0.92
Fe_2O_3	10.46	7.08	8.39	11.29	9.44	9.05	7.46
K_2O	0.03	0.02	0.01	0.06	0.20	0.01	0.01
Na_2O	0.01	0.01	0.01	0.01	0.03	0.01	0.01
P_2O_5	0.02	0.01	0.02	0.02	0.01	0.01	0.01
MnO	0.09	0.11	0.07	0.22	0.13	0.13	0.11
TiO_2	0.02	0.03	0.03	0.05	0.04	0.03	0.03
LOI	12.40	16.70	14.20	15.90	14.20	13.60	16.90
Sum	98.81	98.55	98.75	98.66	99.38	98.75	99.22
Ba (ppm)	4.00	16.00	3.00	74.00	8.00	10.00	9.00
Co	195.60	112.90	128.40	193.30	130.00	192.80	112.10
Cs	0.10	0.20	0.10	0.10	0.10	0.10	0.10
Cu	2.40	12.90	2.60	8.10	12.80	2.50	5.90
Ga	2.50	1.80	2.40	4.00	3.80	2.40	1.40
Hf	0.10	0.10	0.10	0.10	0.10	0.10	0.10
Nb	0.20	0.10	0.20	1.70	1.00	0.60	0.30
Ni	2606.00	2426.00	2636.00	4623.00	2310.00	2481.00	2346.00
Pb	1.60	7.70	0.10	7.60	0.20	0.10	4.30
Rb	0.80	1.10	1.00	3.00	1.10	0.80	0.30
Sc	6.00	4.00	5.00	8.00	6.00	4.00	5.00
Sr	3.50	50.70	1.40	5.70	1.30	1.40	8.80
Ta	0.10	0.10	0.10	0.10	0.10	0.10	0.10
Th	0.20	0.20	0.20	0.20	0.20	0.20	0.20
U	0.10	1.30	10.30	3.00	6.20	10.50	0.10
V	51.00	47.00	41.00	56.00	59.00	33.00	11.00
Y	1.40	1.00	1.60	2.10	1.00	1.50	0.80
Zn	12.00	11.00	23.00	25.00	36.00	24.00	7.00
Zr	6.10	4.30	2.20	6.30	5.00	2.50	2.40
La (ppm)	0.40	1.10	0.70	2.50	0.80	0.70	0.30
Ce	0.70	1.90	0.50	3.90	1.50	0.40	0.70
Pr	0.12	0.21	0.12	0.45	0.22	0.10	0.10
Nd	0.30	1.00	0.30	1.10	1.60	0.50	0.70
Sm	0.13	0.16	0.08	0.38	0.13	0.07	0.15
Eu	0.04	0.10	0.03	0.07	0.07	0.02	0.02
Gd	0.15	0.21	0.13	0.37	0.17	0.08	0.08
Tb	0.04	0.04	0.04	0.07	0.04	0.01	0.03
Dy	0.31	0.20	0.34	0.33	0.28	0.13	0.10
Ho	0.03	0.04	0.04	0.07	0.05	0.02	0.03
Er	0.20	0.12	0.16	0.29	0.18	0.09	0.04
Yb	0.22	0.05	0.08	0.30	0.08	0.11	0.05
Lu	0.05	0.02	0.04	0.04	0.02	0.01	0.01

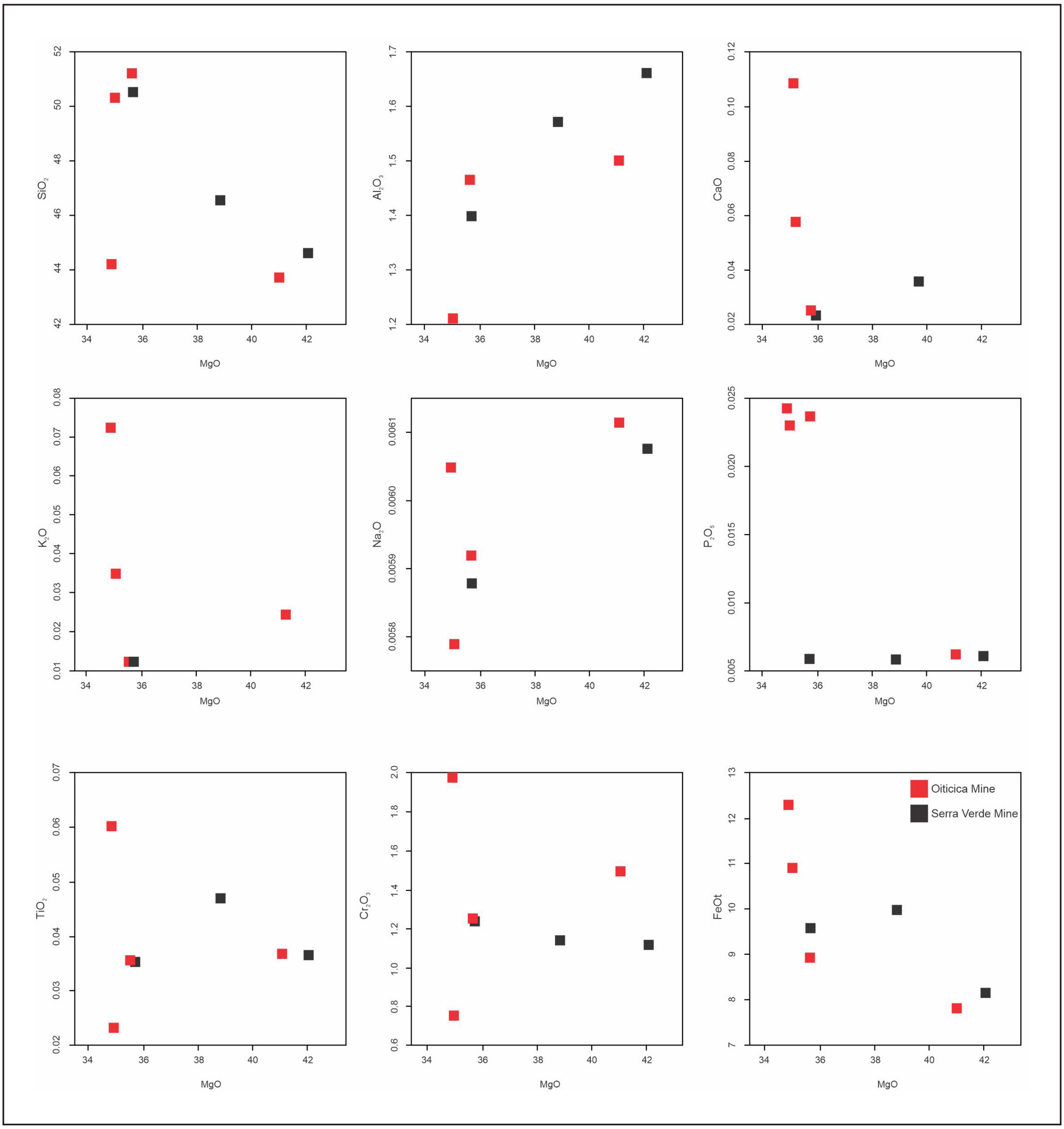

FIGURE 5. Variation diagrams using MgO (wt%) as a differentiation index versus major element oxides (wt%) for the serpentinites from the Serra Verde and Oiticica mines. (Values recalculated on an anhydrous basis).

(Figure 7B) suggest that these rocks may have undergone magmatic differentiation processes or were influenced by hydrothermal fluids enriched in these elements, as the various possible origins for ultramafic rocks typically do not involve significant amounts of these components. The relatively flat REE pattern (Figure 7B) indicates that the rocks may have formed in an environment where rare earth element fractionation processes were not very intense or where equilibrium was maintained during processes such as partial melting or fractional crystallization (Frey et al. 1971; Rollinson 1993).

The similar pattern between the two mines suggests that they may share a common origin or type of geological process. The greater variability in some elements at the Oiticica Mine (such as P and Zr) could indicate a slightly different composition or local variations in the mineral alteration process. Overall, the serpentinites from both locations exhibited similar concentrations of trace elements (LILE, HFSE, and REE) (Figure 7). Despite being less mobile elements, there is significant overlap in the observed values, with no clear differentiation of these samples based on the collection locality.

At the Oiticica Mine, the main product is scheelite ($CaWO_3$), whose genesis was based on the interaction of Brasiliano granitic fluids with the Neoproterozoic metasediments of the Seridó Group (Cavalcanti Neto 1986; Souza Neto et al. 2008;

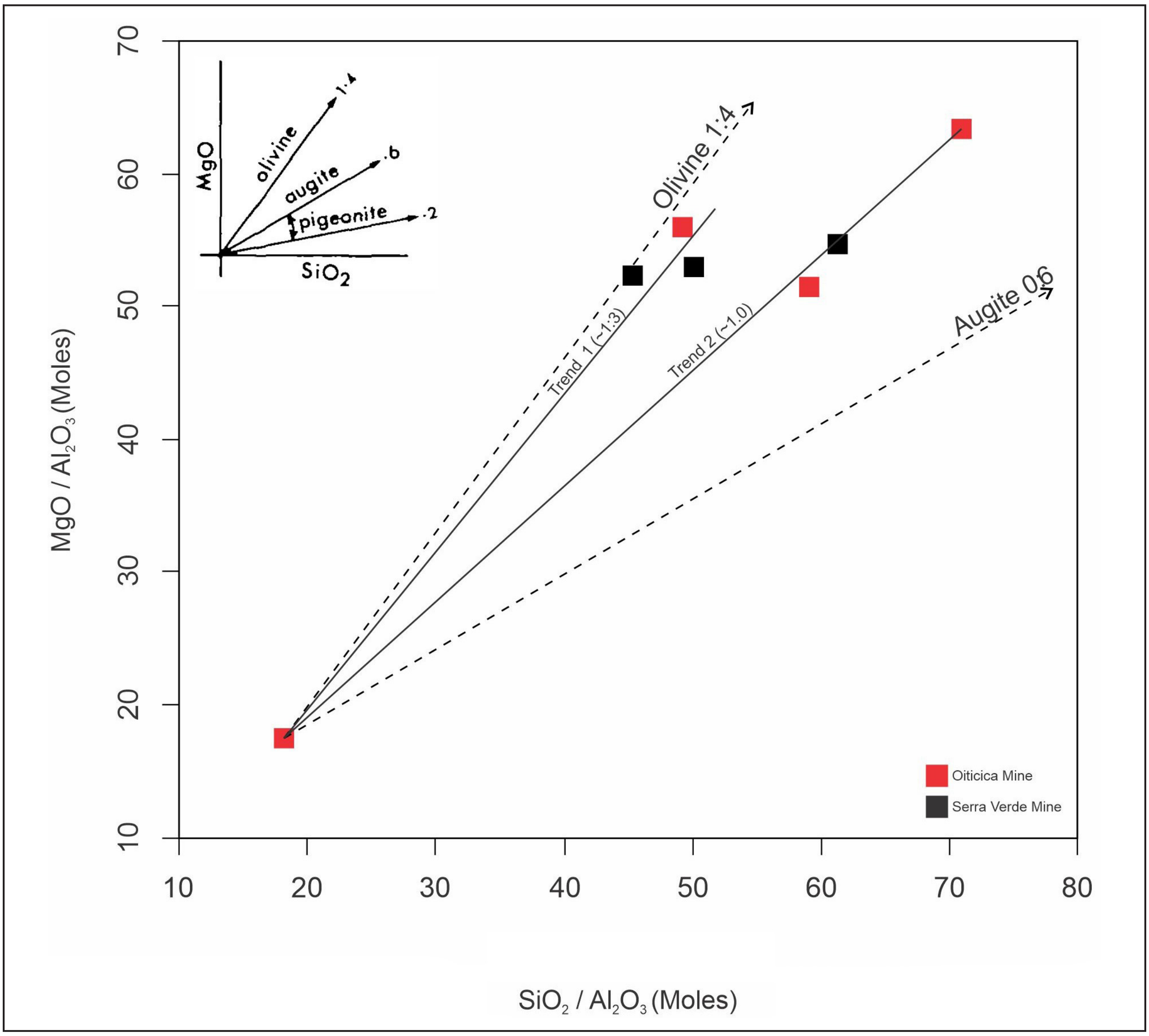

FIGURE 6. MgO/Al_2O_3 vs. SiO_2/Al_2O_3 Diagram (Pearce 1968, 1970) for the studied serpentinites. The arrows indicate the fractionation paths of olivine, augite, and pigeonite, while the lines represent the two trends formed by the analyzed samples.

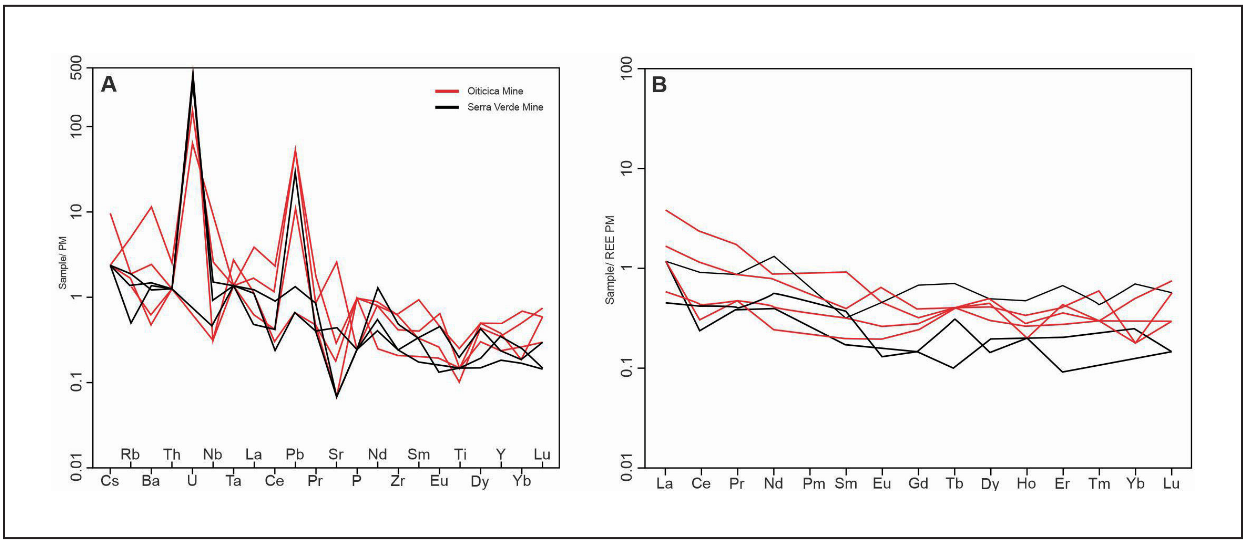

FIGURE 7. A. Trace element patterns normalized to the primitive mantle (PM - McDonough and Sun 1995) for the serpentinites from the Serra Verde and Oiticica mines. B. Rare earth element patterns normalized to chondrites (McDonough and Sun 1995) for the serpentinites from the Serra Verde and Oiticica mines.

Cr from the serpentinite with K, Al, and Be from the pegmatites to create an intermediate phlogopitite layer that hosts the emerald mineralization (Figure 2).

Thus, the understanding of ultramafic bodies near igneous suites is of great importance for opening a new exploration window in a region already well-known for its strong mining tradition.

5.2 Chemical Classification and Genetic Implications

The high MgO and Fe_2O_3 contents, along with low Al_2O_3, TiO_2, and K_2O levels, suggest a komatiitic classification for the studied rocks, following the parameters of Jensen (1976), Viljoen et al. (1982), Le Bas (2000), and Le Maitre (2002) (Figure 8). The absence of spinifex texture (Kerr and Arndt 2001) is understandable and likely erased due to the multiple deformation phases experienced by the rocks in the region.

The average magnesium content in the studied rocks is 31.56%. According to Nisbet (1982), the temperature of komatiitic lavas can be calculated using the equation: Tliquidus = 1400 + [(MgO% - 20) x 20], resulting in a value of 1631.2°C. At this temperature, Bickle et al. (1977) suggest that komatiitic liquids would form at a pressure of approximately 30 kbar. Additionally, Condie (1989) indicates that partial melting under these conditions could range from 35–50%.

The origin of komatiites has, in recent years, sparked significant petrogenetic debate. Various geological environments have been proposed for the emplacement of komatiites, including mid-ocean ridges, plumes, oceanic plateaus, giant meteorite impacts, magma oceans (Grove and Parman 2004), and remnants of plateaus or oceanic arcs (Condie 2001). The most widely accepted model suggests that komatiitic magmas are related to deep mantle plumes without associated volatiles (Campbell et al. 1989). However,

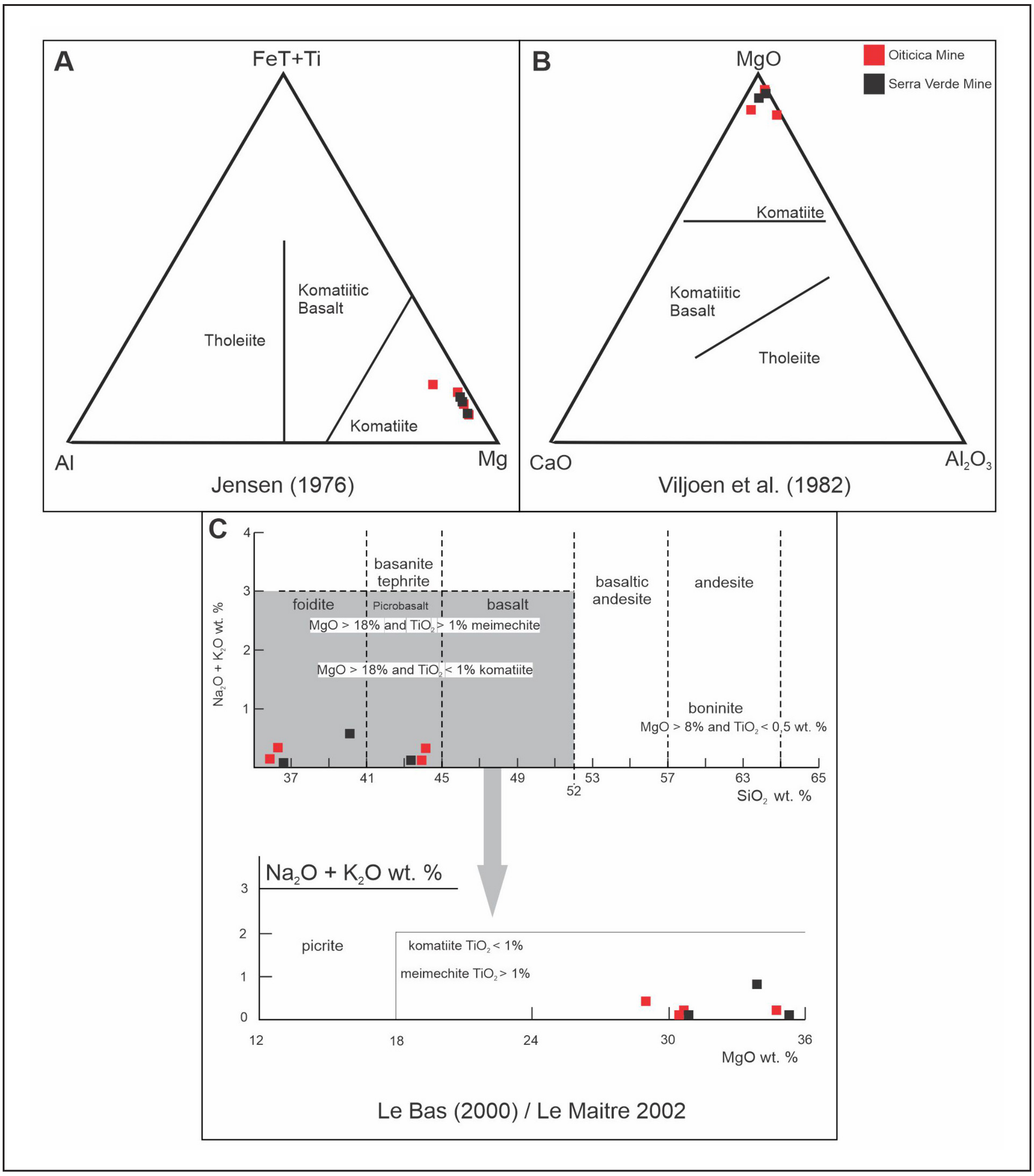

FIGURE 8. Chemical classification of the studied serpentinites according to: A. Jensen (1976); B. Viljoen et al. (1982); C. Le Bas (2000) and Le Maitre (2002).

some researchers propose that komatiites can be produced by hydrated melting at shallow mantle depths in a subduction (arc) environment (Parman et al. 1997; Grove and Parman 2004; Wilson et al. 2003). Nevertheless, there is still no consensus on whether plate tectonics was already active during the Archean.

Models for generating high-MgO magmas, such as komatiites, suggest that these rocks crystallized from nearly anhydrous magmas formed by partial melting of mantle peridotites at temperatures exceeding 1600°C and pressures of approximately 18 GPa (Green 1981; Nisbet et al. 1993). These values are consistent with those found for the serpentinites in the study area and would only be possible under a much higher geothermal gradient than the present, as was characteristic of the Archean Eon.

5.3 Could the Serpentinites be part of a greenstone belt?

Greenstone belts are highly diverse geological entities composed of a wide range of lithologies. Among the various types of volcanic, plutonic, and sedimentary rocks, komatiites and TTGs (tonalite-trondhjemite-granodiorite) stand out, as they were formed under extreme petrogenetic conditions on early Earth and are found in several regions worldwide. Due to their great age and the complex geotectonic environments in which they formed, these rocks typically underwent multiple stages of deformation, metamorphism, and metasomatic alteration, recording a complex tectonic evolution (Anhaeusser 2014).

Santos et al. (2020) identify the serpentinites from the Serra Verde and Oiticica mines as the oldest rocks in South America, with Eoarchean to Paleoarchean ages (3526 and 3747 Ma, U-Pb, SHRIMP). Similarly, Ruiz et al. (2018) report Paleoarchean ages (3506 Ma and 3508 Ma, U-Pb, LA-ICP-MS) in pyroxenites and orthogneisses within the study area. Additionally, Dantas et al. (2004, 2013) and Souza et al. (2015) classify the Mesoarchean to Paleoarchean rocks of the São José do Campestre Domain as a TTG (tonalite-trondhjemite-granodiorite) association (Table 2).

Table 2 - Relationship of Archean rocks in the eastern portion of the Rio Piranhas-Seridó Domain (RPSD) and the São José do Campestre Domain (SJCD), Borborema Province.

Dated rock	**Domain**	**Age (Ma)**	**Method**	**TDM (Ga)**	**Epsilon Nd(t)**	**Reference**
Tonalite	SJCD	3412 ± 8	TIMS, SHRIMP	3.81	-2.24	Dantas et al. (2004)
Granite	SJCD	3356 ± 21	LA-ICP-MS	3.54	+0.34	Souza et al. (2015)
Granite	SJCD	3393 ± 17	LA-ICP-MS	3.66	-1.16	Souza et al. (2015)
Granite	SJCD	3255 ± 4	TIMS, SHRIMP	3.63	-2.39	Dantas et al. (2004)
Tonalite	SJCD	3333 ± 77	SHRIMP	3.27	+1.40	Dantas et al. (2004)
Tonalite	SJCD	3178 ± 8	TIMS, SHRIMP	3.25	+1.20	Dantas et al. (2004)
Granite	SJCD	3118 ± 19	LA-ICP-MS	3.53	-3.21	Souza et al. (2015)
Gabbro	SJCD	3033 ± 3	TIMS, SHRIMP	3.91	-2.87	Dantas (1996)
Granite	SJCD	2685 ± 9	SHRIMP	3.32	-4.20	Dantas et al. (2004)
Amphibolite	SJCD	3447 ± 17	SHRIMP	4.02	-5.0	Dantas et al. (2004)
Amphibolite	RPSD	2657 ± 14	ICPMS-LA			Ferreira et al. (2020a)
Amphibolite	RPSD	2663 ± 16	ICPMS-LA			Ferreira et al. (2020a)
Amphibolite	RPSD	2675 ± 21	ICPMS-LA			Ferreira et al. (2020a)
Amphibolite	RPSD	2692 ± 13	ICPMS-LA			Ferreira et al. (2020a)
Pyroxenite	RPSD	2717 ± 20	ICPMS-LA			Ferreira et al. (2020b)
Migmatite	RPSD	2923 ± 16	ICPMS-LA			Ferreira et al. (2020a)
Orthogneiss	RPSD	3508 ± 16	LA-ICP-MS			Ruiz et al. (2018)
Clinopyroxenite	RPSD	3506 ± 20	LA-ICP-MS			Ruiz et al. (2018)
Serpentinite	RPSD	3747 ± 12	SHRIMP			Santos et al. (2020)
Serpentinite	RPSD	3526 ± 5	SHRIMP			Santos et al. (2020)

Thus, by combining field data with petrography, whole-rock chemistry, and isotopic data available in the literature (Dantas et al. 2004, 2013; Souza et al. 2015; Ruiz et al. 2018; Santiago et al. 2019; Santos et al. 2020), we arrive at a scenario consistent with the studied serpentinites being part of a greenstone belt that was fragmented by the influence of tectonic regimes acting through the Bonfim, Santa Mônica, and São Francisco shear zones.

6. Conclusion

Based on the acquired data, our study of the serpentinites from the Rio Piranhas-Seridó Domain indicates that:

- The serpentinites occur as small, elongated bodies in contact with the metasediments of the Seridó Group and the gneiss-migmatites of the Caicó Complex. They are melanocratic, fine-grained rocks with a greenish color, serpentine as the primary phase, and chlorite, magnetite, muscovite, and tremolite as accessory minerals.
- Rock analyses revealed SiO_2 values ranging from 35.72% to 43.48%, MgO > 28.88%, Fe_2O_3 between 7.08% and 11.29%, Al_2O_3 < 3.42%, with very low concentrations of TiO_2, CaO, K_2O, and Na_2O.
- No direct relationship was found between scheelite mineralization (Oiticica Mine) and the serpentinite, unlike at the Serra Verde Mine, where the genesis of emeralds is conditioned by the presence of this ultramafic rock.
- Ultramafic rocks are associated with significant mineral deposits worldwide, and advancing studies may lead to new discoveries in a region already renowned for its strong mining tradition.
- Temperature, pressure, and partial melting conditions align with bibliographic data, supporting the interpretation that the studied serpentinites are part of a greenstone belt.

Acknowledgments

We thank CNPq for providing financial support for fieldwork and chemical analyses through project number 1533695260888392, granted to MTOCN. We also extend our gratitude to UFPE and IFRN for providing infrastructure and logistical support. Special thanks to CAPES (Coordination for the Improvement of Higher Education Personnel) for financial support to the PPGEOC/UFPE (Graduate Program in Geosciences). F.G. Santos is grateful to the Geological Survey of Brazil (CPRM) for encouraging the pursuit of a Master's degree in Geology. Finally, we thank the reviewers of JGSB, Guilherme Ínsua-Pereira and an anonymous reviewer, for their constructive comments.

Authorship credits

Author	A	B	C	D	E	F
FGS	■	■	■	■	■	
MTOCN		■			■	
VPF		■			■	■
ALB		■			■	

A - Study design/ Conceptualization
B - Investigation/ Data acquisition
C - Data Interpretation/ Validation
D - Writing
E - Review/Editing
F - Supervision/Project administration

References

Almeida F.F.M., Hasui Y., Brito Neves B.B., Fuck R.A. 1981. Brazilian structural provinces: an introduction. Earth-Science Reviews, 17(1-2), 1-29. https://doi.org/10.1016/0012-8252(81)90003-9

Angelim L.A.A., Medeiros V.C., Nesi J.R. 2006. Mapa geológico do estado do Rio Grande do Norte, Escala 1:500.000. Programa Geologia do Brasil, Recife, CPRM, FAPERN. Available online at: https://rigeo.sgb.gov.br/bitstream/doc/10234/2/Mapa_Rio_grande_norte.pdf / (accessed on 27 November 2024).

Anhaeusser C.R. 2014. Archaean greenstone belts and associated granitic rocks - a review. Journal of African Earth Sciences 100, 684–732. https://doi.org/10.1016/j.jafrearsci.2014.07.019

Arthaud M.H., Caby R., Fuck R.A., Dantas E.L., Parente C.V. 2008. Geology of the Northern Borborema Province, NE Brazil and its correlation with Nigeria, NW Africa. In: Pankhurst R.J., Trouw R.A.J., Brito Neves B.B., De Wit M.J. (org.). West Gondwana: Pre-Cenozoic correlations across the South Atlantic Region. Geological Society of London Special Publications, 294(1), 49–67. http://dx.doi.org/10.1144/SP294.4

Bickle M.J., Ford C.E., Nisbet E.G. 1977. The petrogenesis of peridotitic komatiites: evidence from high-pressure melting experiments. Earth and Planetary Science Letters, 37(1), 97-106. https://doi.org/10.1016/0012-821X(77)90150-9

Bogolepov V.G. 1970. Problem of serpentinization of ultrabasic rocks. International Geology Review, 12(4), 421-432. https://doi.org/10.1080/00206817009475250

Brito Neves B.B., Santos E.J., Van Schmus W.R. 2000. Tectonic history of the Borborema Province, Northeastern Brazil. In: Cordani U., Milani E.J., Thomaz Filho A., Campos D.A. (eds.). Tectonic evolution of South America. Rio de Janeiro, International Geological Congress, 31, p. 151–182. Available online at: https://rigeo.sgb.gov.br/handle/doc/19419 / (accessed on 27 November 2024).

Caby R. 1989. Precambrian terranes of Benin-Nigeria and northeast Brazil and the late Proterozoic south Atlantic fit. In: Dallmeyer R.D. (ed.). Terranes in the Circum-Atlantic Paleozoic Orogens. Special Papers, Geological Society of America, 230, p. 145-158. https://doi.org/10.1130/SPE230-p145

Campbell I.H., Griffiths R.W., Hill R.I. 1989. Melting in an Archean mantle plume: heads it is basalts, tails it is komatiites. Nature, 339, 697-699. http://dx.doi.org/10.1038/339697a0

Cavalcanti Neto M.T.O. 1986. Geologia da área de Brejuí e São Sebastião, Currais Novos-RN: geologia da mina Brejuí e anexos. Graduation work, Departamento de Geologia, Universidade Federal do Rio Grande do Norte, 422 p.

Coleman R.G., Keith T.E. 1971. A chemical study of serpentinization – Burro Mountain, California. Journal of Petrology, 12(2), 311-328. https://doi.org/10.1093/petrology/12.2.311

Condie K.C. 1989. Magma Associations and Mantle Souces. In: Condie K.C. (ed.). Plate Tectonics & Crustal Evolution. 3rd edition. Oxford, Pergamon, p. 208-243.

Condie K.C. 2001. Mantle Plumes and their Record in Earth history. Cambridge, Cambridge University Press, 306 p. https://doi.org/10.1017/CBO9780511810589

Dantas E.L. 1996. Geocronologia U-Pb e Sm-Nd de terrenos arqueanos e paleoproterozóicos do Maciço Caldas Brandão, NE do Brasil. PhD Thesis, Instituto de Geociências e Ciências Exatas, Universidade Estadual Paulista, Rio Claro, 206 p.

Dantas E.L., Van Schmus W.R., Hackspacher P.C., Fetter A.H., Brito Neves B.B., Cordani U., Nutman A.P., William I.S. 2004. The 3.4–3.5 Ga São José do Campestre massif, NE Brazil: remnants of the oldest crust in South America. Precambrian Research, 130(1-4), 113–137. https://doi.org/10.1016/j.precamres.2003.11.002

Dantas E.L., Souza Z.S., Wernick E., Hackspacher P.C., Xiaodong D., Li J.W. 2013. Crustal growth in the 3.4-2.7Ga São José de Campestre Massif, Borborema province, NE Brazil. Precambrian Research, 227, 120–156. https://doi.org/10.1016/j.precamres.2012.08.006

De Wit M.J., Ashwal L.D. 1997. Preface: Convergence towards divergent models of greenstone belts. In: De Wit M.J., Ashwal L.D. (eds.). Greenstone Belts. Oxford, Oxford University Press, p. 9-17.

Delgado I.M., Souza J.D., Silva L.C., Silveira Filho N.C., Santos R.A., Pedreira A.J., Guimarães J.T., Angelim L.A.A., Vasconcelos A.M., Gomes I.P., Lacerda Filho J.V., Valente C.R., Perrota M.M., Heineck C.A. 2003. Geotectônica do Escudo Atlântico. In: Bizzi L.A., Schobbenhaus C., Vidotti R.M., Gonçalves J.H. Geologia, tectônica e recursos minerais do Brasil. Brasília, CPRM, p. 227-334. Available online at: https://rigeo.sgb.gov.br/handle/doc/5006 / (accessed on 27 November 2024).

Deschamps F., Godard M., Guillot S., Hattori K. 2013. Geochemistry of subduction zone serpentinites: A review. Lithos, 178, 96–127. https://doi.org/10.1016/j.lithos.2013.05.019

Dostal J. 2008. Komatiites. Geoscience Canada. 35(1), 21-31. Available online at: https://id.erudit.org/iderudit/geocan35_1ser02 / (accessed on 2 December 2024).

Evans B.W., Hattori K., Baronnet A. 2013. Serpentinites: What, why, where? Elements, 9(2), 99-106. https://doi.org/10.2113/gselements.9.2.99

Ferreira A.C.D., Dantas E.L., Fuck A.R., Nedel I.M. 2020a. Arc accretion and crustal reworking from late Archean to Neoproterozoic in Northeast Brazil. Scientific Reports, 10(1), 7855. https://doi.org/10.1038/s41598-020-64688-9

Ferreira A.C.D., Dantas E.L., Santos T.J.S., Fuck R.A., Tedeschi M. 2020b. High-pressure metamorphic rocks in the Borborema Province, Northeast Brazil: reworking of archean oceanic crust during proterozoic orogenies. Geoscience Frontiers, 11(6), 2221-2241. https://doi.org/10.1016/j.gsf.2020.03.004

Frey F.A., Haskin L.A., Haskin M.A. 1971. Rare-Earth abundances in some ultramafic rocks. Journal of Geophysical Research, 76(8), 2057-2070. https://doi.org/10.1029/JB076i008p02057

Green D.H. 1981. Petrogenesis of Archaean ultramafic magmas and implications for Archaean tectonics. In: Kröner A. (ed.). Precambrian plate tectonics. Developments in Precambrian Geology, Elsevier, Amsterdam, 4, p. 469-489. https://doi.org/10.1016/S0166-2635(08)70024-0

Grove T.L., Parman S.W. 2004, Thermal evolution of the Earth as recorded by komatiites. Earth and Planetary Science Letters, 219(3-4), 173-187. https://doi.org/10.1016/S0012-821X(04)00002-0

Hollanda M.H.B.M., Souza Neto J.A., Archanjo C.J., Stein H., Maia A.C.S. 2017. Age of the granitic magmatism and the W-Mo mineralizations in skarns of the Seridó belt (NE, Brazil) based on zircon U-Pb (SHRIMP) and molybdenite Re-Os dating. Journal of South American Earth Sciences, 79, 1-11. https://doi.org/10.1016/j.jsames.2017.07.011

Jardim de Sá E.F. 1994. A Faixa Seridó (Província Borborema, NE do Brasil) e seu significado geodinâmico na Cadeia Brasiliana / Pan Africana. PhD Thesis, Instituto de Geociências, Universidade de Brasília, Brasília, 804 p.

Jensen L.S. 1976. A new cation plot for classifying subalkaline volcanic rocks. Miscellaneous Paper, Toronto, Ontario Division of Mines, 66, 1-22.

Kerr A.C., Arndt N.T. 2001. A note on the IUGS reclassification of the high-Mg and picritic volcanic rocks. Journal of Petrology, 42(11), 2169-2171. https://doi.org/10.1093/petrology/42.11.2169

Le Bas M.J. 2000. IUGS reclassification of the high-Mg and picritic volcanic rocks. Journal of Petrology, 41(10), 1467–1470. https://doi.org/10.1093/petrology/41.10.1467

Le Maitre R.W. 2002. Igneous rocks: a classification and glossary of terms. 2nd edition. Cambridge, Cambridge University Press, 236 p. https://doi.org/10.1017/CBO9780511535581

McDonough W.F., Sun S.S. 1995. The composition of the earth. Chemical Geology, 120(3-4), 223-253. http://dx.doi.org/10.1016/0009-2541(94)00140-4

Medeiros V.C., Cavalcante R., Cunha A.L.C., Dantas A.R., Costa A.P., Brito A.A., Rodrigues J.B., Silva M.A. 2017. O furo estratigráfico de Riacho Fechado (Currais Novos/RN), domínio Rio Piranhas-Seridó (província Borborema, NE Brasil): procedimentos e resultados. Estudos Geológicos, 27(3), 3-44. https://doi.org/10.18190/1980-8208/estudosgeologicos.v27n3p1-40

Nascimento M.A.L., Galindo A.C., Medeiros V.C. 2015. Ediacaran to Cambrian magmatic suites in the Rio Grande do Norte domain, extreme Northeastern Borborema Province (NE of Brazil): current knowledge. Journal of South American Earth Sciences, 58, 281-299. http://dx.doi.org/10.1016/j.jsames.2014.09.008

Neves S.P. 2015. Constrains from zircon geochronology on the tectonic evolution of the Borborema Province: Widespread intracontinental Neoproterozoic reworking of a Paleoproterozoic accretionary orogen. Journal of South American Earth Sciences, 58, 150-164. https://doi.org/10.1016/j.jsames.2014.08.004

Nisbet E.G. 1982. The tectonic setting and petrogenesis of Komatiites. In: Arndt N.T., Nisbet E.G. (eds.). Komatiites. London, George Allen and Unwin, p. 501-526.

Nisbet E.G., Cheadle M.J., Arndt N.T., Bickle M.J. 1993. Constraining the potential temperature of the Archean mantle: A review of evidence from komatiites. Lithos, 30(3-4), 291-307. https://doi.org/10.1016/0024-4937(93)90042-B

O'Hanley D.S. 1996. Serpentinites, records of tectonic and petrological history. Monographs on Geology and Geophysics, New York, Oxford University Press, 34, 277 p.

Parman S.W., Dann J.C., Grove T.L., De Wit M.J. 1997. Emplacement conditions of komatiite magmas from the 3.49 Ga Komati Formation, Barberton Greenstone Belt, South Africa. Earth Planetary Science Letters, 150(3-4), 303-323. https://doi.org/10.1016/S0012-821X(97)00104-0

Pearce T.H. 1968. A contribution to the theory of variation diagrams. Contributions to Mineralogy and Petrology, 19, 142–157. https://doi.org/10.1007/BF00635485

Pearce T.H. 1970. Chemical Variations in the Palisade Sill. Journal of Petrology, 11(1),15-32. https://doi.org/10.1093/petrology/11.1.15

Pitombeira J.P.A., Amaral W.S., Uchôa Filho E.C., Fuck R.A., Dantas E.L., Parente C.V., Costa F.G., Verissimo C.U.V. 2016. Vestiges of a continental margin ophiolite type in the Novo Oriente region, Borborema Province, NE Brazil. Journal of South American Earth Sciences, 73, 78-99. https://doi.org/10.1016/j.jsames.2016.11.007

Rollinson H.R. 1993. Using geochemical data: evaluation, presentation, interpretation. London, Longman Scientific and Technical, 315 p. Available online at: https://www.sbgeo.org.br/books/Rollinson 1993.pdf / (accessed on 3 December 2024).

Ruiz F.V., Della Giustina M.E.S., Oliveira C.G., Dantas E.L., Hollanda M.H.B. 2018. The 3.5 Ga São Tomé layered mafic-ultramafic intrusion, NE Brazil: Insights into a Paleoarchean Fe-Ti-V oxide mineralization and its reworking during West Gondwana assembly. Precambrian Research, 326, 462-478. http://dx.doi.org/10.1016/j.precamres.2018.03.011

Santiago J.S., Souza V.S., Filgueiras B.C., Jiménez F.A.C. 2019. Emerald from the Fazenda Bonfim Deposit, northeastern Brazil: chemical, fluid inclusions and oxygen isotope data. Brazilian Journal of Geology, 48(3), 457-472. https://doi.org/10.1590/2317-4889201820170130

Santos E.J., Souza Neto J.A., Silva M.R.R., Beurlen H., Cavalcanti J.A.D., Silva M.G., Costa A.F., Santos L.C.M.L., Santos R.B. 2014. Metalogênese das porções norte e central da Província Borborema. In: Silva M.G., Neto M.B.R., Jost H., Kuyumijan R.M. (eds.). Metalogênese das Províncias Tectônicas Brasileiras. Belo Horizonte, CPRM, p. 343-388. Available online at: https://rigeo.sgb.gov.br/jspui/bitstream/doc/19389/1/metalogenese_provincias_tectonicas_brasileiras.pdf / (accessed on 28 November 2024).

Santos F.G., Cavalcanti Neto M.T.O., Ferreira V.P., Bertotti A.L. 2020. Eo to Paleoarchean metamafic-ultramafic rocks from the central portion of the Rio Grande do Norte Domain, Borborema Province, northeast Brazil: the oldest South American platform rock. Journal of South American Earth Sciences, 97, 102410. https://doi.org/10.1016/j.jsames.2019.102410

Souza Z.S., Martin H., Peucat J.J., Jardim de Sá E.F., Macedo M.H.F. 2007. Calc-Alkaline Magmatism at the Archean-Proterozoic Transition: the Caicó Complex Basement (NE Brazil). Journal of Petrology, 48(11), 2149–2185. https://doi.org/10.1093/petrology/egm055

Souza Z.S., Kalsbeek F., Deng X., Frei R., Kokfelt T.F., Dantas E.L., Li J., Pimentel M.M., Galindo A.C. 2015. Generation of continental crust in the northern part of the Borborema Province, northeastern Brazil, from Archaean to Neoproterozoic. Journal of South American Earth Sciences, 68, 68-96. https://doi.org/10.1016/j.jsames.2015.10.006

Souza Neto J.A., Legrand J.M., Volfinger M., Pascal M., Sonnet P. 2008. W–Au skarns in the Neo-Proterozoic Seridó Mobile Belt, Borborema Province in northeastern Brazil: an overview with emphasis on the Bonfim deposit. Mineralium Deposita, 43, 185-205. http://dx.doi.org/10.1007/s00126-007-0155-1

Szilas K., Van Hinsberg V.J., Creaser R.A., Kisters A.F.M. 2014. The geochemical composition of serpentinites in the Mesoarchaean Tartoq Group, SW Greenland: Harzburgitic cumulates or melt-modified mantle? Lithos, 198-199, 103-116. https://doi.org/10.1016/j.lithos.2014.03.024

Uchoa Filho E.C., Amaral W.S., Pitombeira J.P.A., Parente C.V. 2014. Petrografia da sequência metaultramáfica de Novo Oriente – CE: vestígios de um ofiolito transicional ou uma margem passiva pobre em magma. Revista de Geologia UFC, 27(1), 19-37. Available online at: http://www.periodicos.ufc.br/geologia/article/view/1289 / (accessed on 28 November 2024).

Van Schmus W.R., Brito Neves B.B., Willians I.S., Hackspacher P.C., Fetter A.H., Dantas E.L., Babinski M. 2003. The Seridó Group of NE Brazil, a late Neoproterozoic pre- to syn-collisional basin in West Gondwana: insights from SHRIMP U-Pb detrital zircon ages and Sm-Nd crustal residence (TDM) ages. Precambrian Research, 127(4), 287–327. https://doi.org/10.1016/S0301-9268(03)00197-9

Viljoen M.J., Viljoen R.P., Pearton T.N. 1982. The nature and distribution of Archaean komatiite volcanics in South Africa In: Arndt N.T., Nisbet E.G. Komatiites. London, Allen and Unwin, p. 53-79.

Wilson A.H., Shirey S.B., Carlson R.W. 2003. Archean ultra-depleted komatiites formed by hydrous melting of cratonic mantle. Nature, 423, 858-861. https://doi.org/10.1038/nature01701

Zwaan J.C., Jacob D.E., Häger T., Cavalcanti Neto M.T.O., Kanis J. 2012. Emeralds from the Fazenda Bonfim Region, Rio Grande do Norte, Brazil. Gems and Gemology, 48(1), 2-17. http://dx.doi.org/10.5741/GEMS.48.1.2